Energy Treated ascorbic acid was calculated compared with the control ascorbic acid using the following equation 2:

$$\% \text{ change} = \frac{[\text{Treated} - \text{Control}]}{\text{Control}} \times 100 \quad (2)$$

RESULTS AND DISCUSSION

Powder x-ray diffraction (PXRD) analysis

The PXRD study showed the diffractograms of the control and treated samples **(Figure 1)** from which the further analysis was done by comparing the relative intensity and the crystallite sizes of the characteristic peaks **(Table 1)** of both the samples. There was the presence of sharp and intense peaks in the diffractograms of the control and treated samples, which indicated their crystalline nature. However, there were some alterations in the Bragg's angles of the characteristic peaks of the treated sample as compared to the control sample that denoted the impact of the Biofield Energy Treatment on the crystalline properties of ascorbic acid.

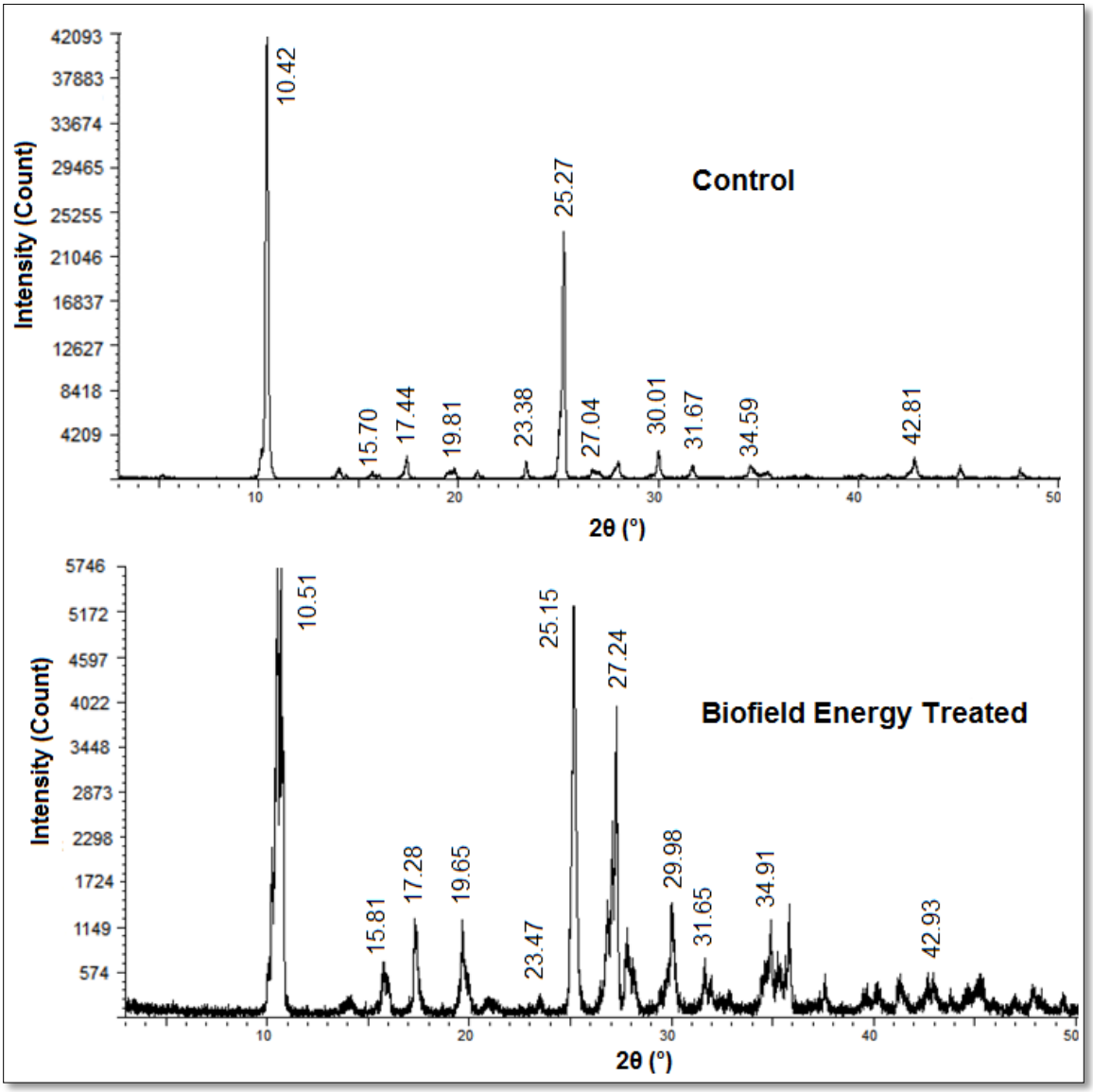

Figure 1. PXRD diffractograms of the control and treated ascorbic acid.

Table 1. PXRD data for the control and treated ascorbic acid.

Entry No.	Bragg angle (°2θ)		Intensity (cps)			Crystallite size (G, nm)		
	Control	Treated	Control	Treated	% change	Control	Treated	% change
1	10.42	10.51	1345	632	-53.01	195	513	163.08
2	15.70	15.81	55	129	134.55	535	382	-28.60
3	17.44	17.28	290	184	-36.55	436	333	-23.62
4	19.81	19.65	59	239	305.08	645	482	-25.27
5	23.38	23.47	165	37	-77.58	695	449	-35.40
6	25.27	25.15	1949	928	-52.39	831	950	14.32
7	27.04	27.24	76	356	368.42	439	771	75.63
8	30.01	29.98	370	164	-55.68	672	388	-42.26
9	31.67	31.65	196	65	-66.84	494	545	10.32
10	34.59	34.91	193	72	-62.69	425	800	88.24
11	42.81	42.93	210	69	-67.14	598	661	10.54

The analysis of the peak intensities and crystallite sizes corresponding to the characteristic peaks of the treated sample showed some significant changes, as the relative intensities were altered ranging from -77.58% to 368.42%; while the crystallite sizes were changed ranging from -42.26% to 163.08%, in comparison to the control sample. The impact of the Biofield Energy Treatment was also visible on the average crystallite size, as it was increased by 5.18% in the treated sample (570.36 nm) as compared to the control sample (542.27 nm). The previous studies signify the impact of altered peak intensities and crystallite size on the crystalline properties of the sample in terms of changes in the crystal morphology that might indicate the formation of novel polymorph [37,38] of the treated ascorbic acid. Such techniques of changing the crystal properties and habit could be used in improving the efficacy and bioavailability of the compound [39]. Hence, it is presumed that the treated ascorbic acid sample might form a new polymorph that might show improved efficacy and bioavailability after the Biofield Energy Treatment compared to the untreated sample.

Particle size analysis (PSA)

The particle size analysis of both the samples helps in analysing the effect of the Biofield Energy Treatment on the particle size distribution of the ascorbic acid corresponding at d10, d50, d90 and D(4, 3) in comparison to the untreated sample **(Table 2)**. The results indicated the particle size distributions of the treated sample were significantly increased by 12.67% (d10), 29.60% (d50), 18.29% (d90), and 22.35% {D(4, 3)} as compared to the control sample.

Table 2. Particle size distribution of the control and treated ascorbic acid.

Parameters	d_{10} (µm)	d_{50} (µm)	d_{90} (µm)	D(4,3) (µm)	SSA (m^2/g)
Control	71.58	245.20	556.72	283.13	0.043
Biofield Treated	80.65	317.78	658.56	346.41	0.037
Percent change (%)	12.67	29.60	18.29	22.35	-13.95

SSA: The specific surface area: d_{10}, d_{50} and d_{90}: particle diameter corresponding to 10%, 50% and 90% of the cumulative distribution, D(4,3): the average mass-volume diameter

The resultant specific surface area of the treated sample (0.037 m^2/g) was significantly reduced by 13.95% due to the increase in the particle size, as compared to the control sample (0.043 m^2/g). Various scientific studies specified the effect of the particle size distribution of the formulation criteria of the drug such as its compactibility, blend uniformity and flowability, etc. Such properties further affect the efficacy, safety, stability, and quality control of the nutraceutical/pharmaceutical formulation [40,41]. The treated ascorbic acid sample might show better flowability, content uniformity, and compactibility after the Biofield Energy Treatment in comparison to the control sample.

Thermal gravimetric analysis (TGA)/differential thermogravimetric analysis (DTG)

The impact of heat on the stability profile of the control and treated ascorbic acid samples were analysed along with its degradation pattern by the TGA/DTG technique. The scientific literature reported the stability of ascorbic acid till ~200°C when heated and afterward the degradation started leaving the non-decomposed and carbonaceous residues of ascorbic acid in the form of residual mass [42]. The TGA analysis data of the control and treated samples **(Figure 2)** also indicated the stability of samples till 200°C as reported in scientific literature. The total weight loss of the treated ascorbic acid sample was decreased significantly by 8.23% during the thermal heating, as it was observed to be 76.04% as compared to the control sample (82.86%). The significant reduction in weight loss of the treated sample contributed to the remarkable increase in the residue amount by 39.79% after the thermal degradation **(Table 3)** in comparison to the control sample's residue. Thus, it showed the increased thermal stability and reduced degradation of the treated sample compared to the control sample.

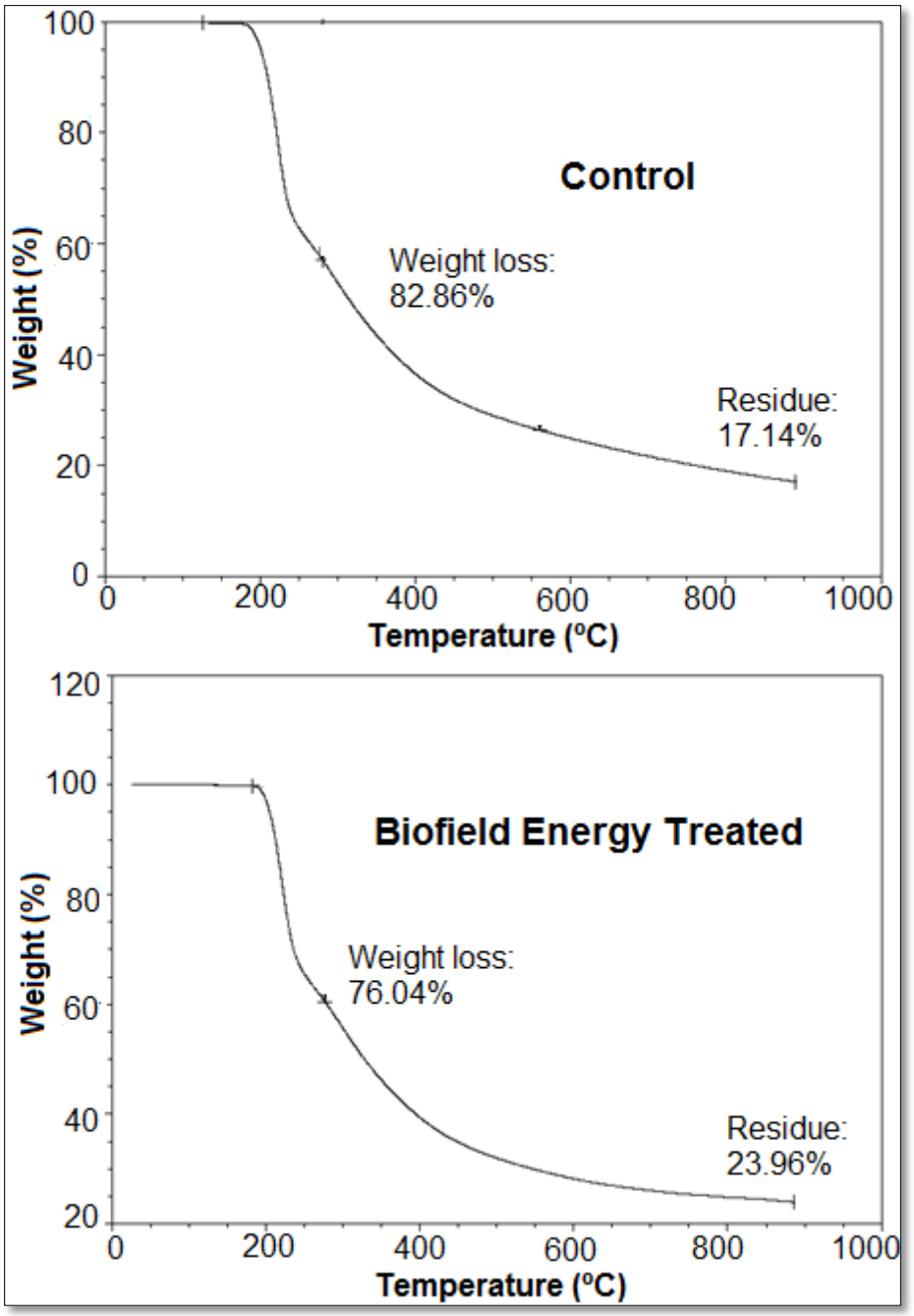

Figure 2. TGA thermograms of the control and treated ascorbic acid.

Table 3. TGA/DTG data of the control and treated samples of ascorbic acid.

Samples	TGA		DTG; T_{max} (°C)	
	Total weight loss (%)	Residue %	Peak 1	Peak 2
Control	82.86	17.14	222.42	314.07
Biofield Energy Treated	76.04	23.96	220.09	317.38
% Change	-8.23	39.79	-1.05	1.05

T_{max} = the temperature at which maximum weight loss takes place in TG or peak temperature in DTG

Moreover, the DTG data indicated the two peaks in the thermograms of both the samples **(Figure 3)** that denoted the temperature (T_{max}) at which maximum thermal degradation has taken place. The treated sample's thermogram showed Tmax at 220.09°C and 317.38°C for the 1st and 2nd peak, respectively in comparison to the T_{max} of the control sample that was observed at 222.42°C and 314.07°C, respectively. Thus, the treated sample showed 1.05% decrease in the T_{max} of the 1st peak, while the 2nd peak was increased by 1.05% as compared to the control sample. Hence, the study indicated the increased thermal stability of the treated sample at higher temperature range as compared to the control ascorbic acid sample. The overall TGA/DTG studies revealed the significant reduction in the thermal degradation of the treated sample that indicated the increased thermal stability of the ascorbic acid after the Biofield Energy Treatment.

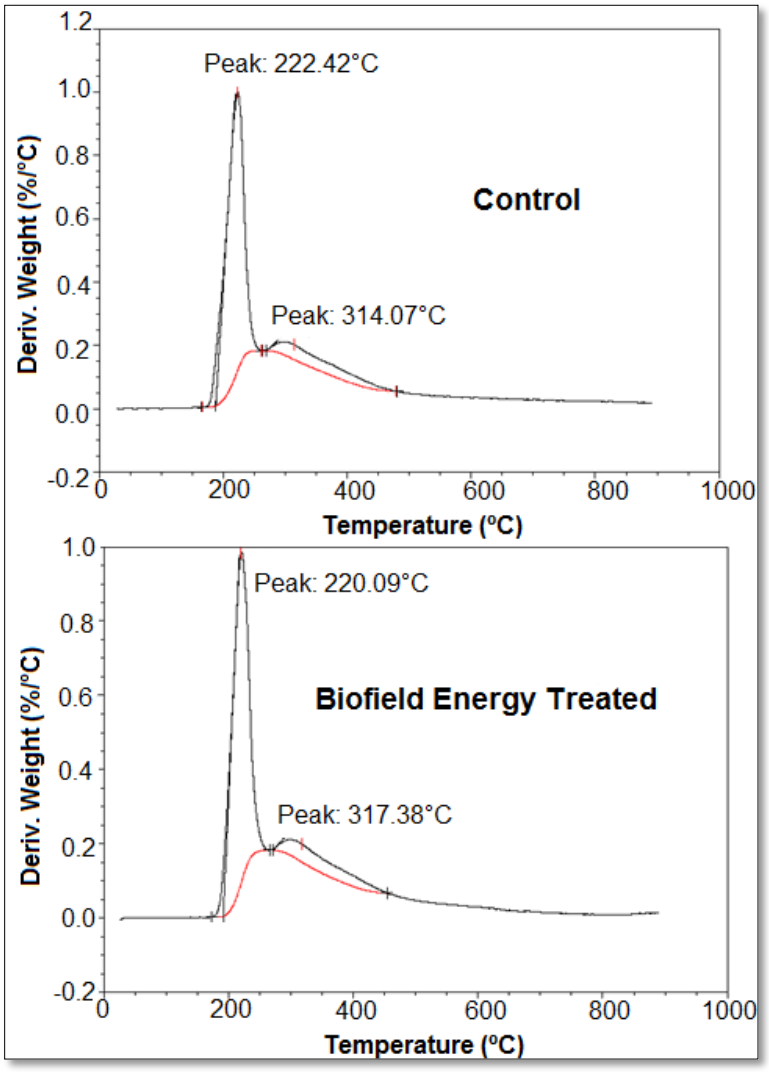

Figure 3. DTG thermograms of the control and treated ascorbic acid.

Differential scanning calorimetry (DSC) analysis

The DSC analysis helps in analysing the difference between the control and treated ascorbic acid sample in terms of their melting and decomposition temperatures along with the latent heat used during the process in the process of heating [43]. The scientific studies reported the presence of an endothermic peak (melting peak) at 193°C in the DSC thermogram of ascorbic acid when heated at the rate of 10°C/min. Moreover, an exothermic peak was also reported in the thermogram that is considered as the thermal decomposition of the ascorbic acid during its further heating that resulted in the release of the volatile compounds thereby forming the carbonaceous residue [42]. The DSC thermograms of the control and the treated samples **(Figure 4)** were observed similarly as mentioned in the previous studies. The further analysis reported that the treated sample showed the endothermic peak with minor increase in the melting temperature (0.42%), while the ΔH_{fusion} was increased by 7.63% **(Table 4)** as compared to the control sample. Besides, the exothermic peak (decomposition temperature) of the treated sample was present at 215.14°C, which was decreased by 7.60% (~17°C) in comparison to the degradation temperature of the control sample. Also, the treated sample showed a reduction in the $\Delta H_{decomposition}$ by 12.96%, compared to the control ascorbic acid sample **(Table 4)**.

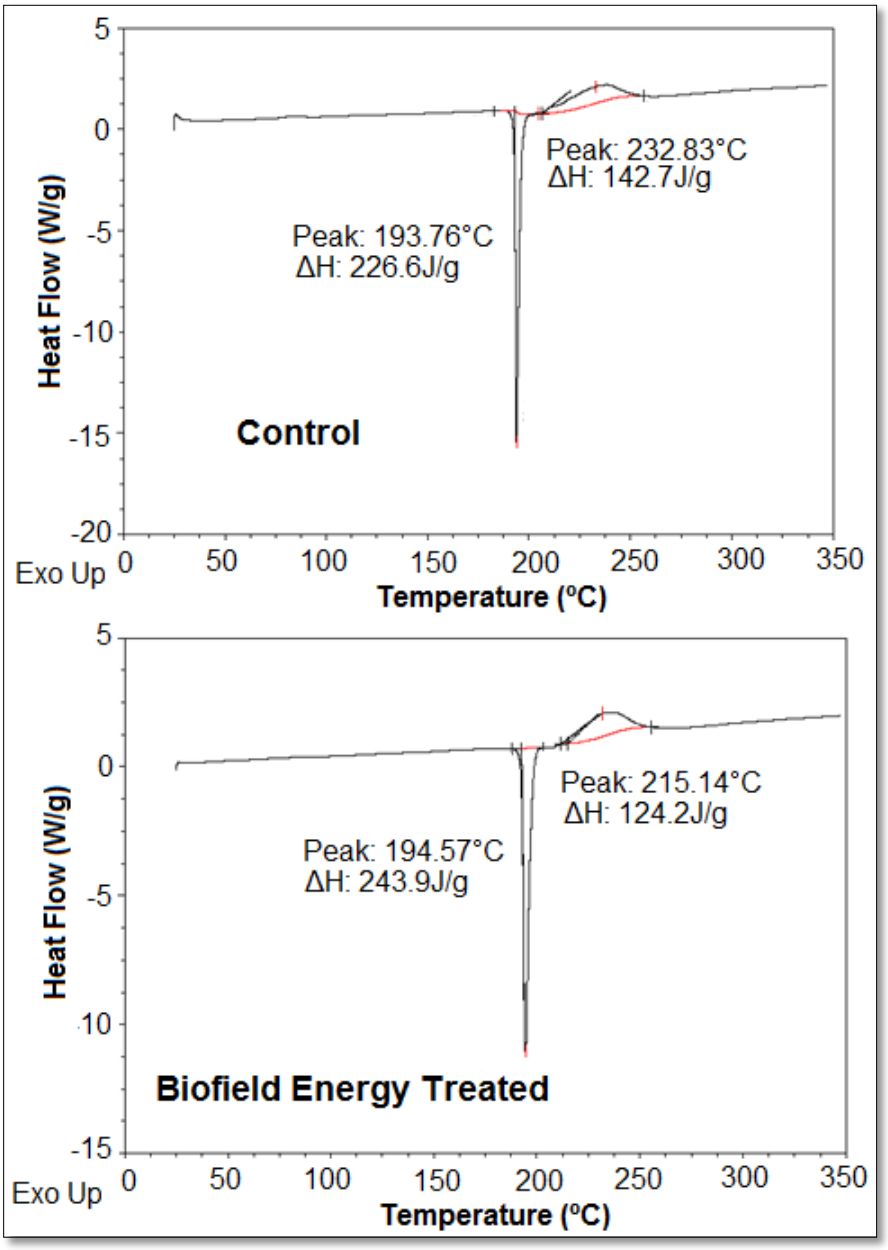

Figure 4. DSC thermograms of the control and treated ascorbic acid.

Table 4. Comparison of DSC data between the control and treated ascorbic acid.

Peaks	Description	Melting Point (°C)	ΔH (J/g)
Peak 1	Control sample	193.76	226.60
	Biofield Treated sample	194.57	243.90
	% Change	0.42	7.63
Peak 2	Control sample	232.83	142.70
	Biofield Treated sample	215.14	124.20
	% Change	-7.60	-12.96

ΔH: Latent heat of fusion and decomposition

Hence, the overall DSC data revealed the significant decrease in the decomposition temperature along with remarkable alterations in ΔH_{fusion} and $\Delta H_{decomposition}$ of the treated sample after the Biofield Energy Treatment that might indicate some changes in the crystallization structure and molecular bonding [43] of the ascorbic acid in comparison to the control sample.

CONCLUSION

The study concluded the outcome of the Trivedi Effect®-Consciousness Energy Healing Treatment on the crystalline, physical and thermal properties of ascorbic acid in comparison to the untreated sample. The PXRD peak intensities of the treated sample and the corresponding crystallite sizes showed changes ranging from -77.58% to 368.42% and -42.26% to 163.08%, respectively as compared to the control sample. Besides, the treated sample showed an increase in the average crystallite size by 5.18% compared with the control ascorbic acid sample. Such significant changes in the treated sample might be attributed to the polymorphic transition of the ascorbic acid sample that may take place after the Biofield Energy Treatment in comparison to the untreated ascorbic acid sample. The new polymorph of the treated ascorbic acid might show better bioavailability and efficacy compared to the control sample. The particle size data indicated the significant changes in the particle size distribution of the treated sample corresponding to d10, d50, d90, and D(4,3) that were observed to be increased by 12.67%, 29.60%, 18.29% and 22.35%, respectively, compared to the control sample. The significant increase in the particle sizes of the treated ascorbic acid sample contributed to the decrease in the specific surface area by 13.95% compared with the control sample. Such alterations in the particle sizes of the treated sample might improve the appearance, flowability and content uniformity of ascorbic acid during the formulation development as compared to the untreated sample. The weight loss of the treated sample was 8.23% decreased, but the residue weight was significantly increased by 39.79% compared with the control sample. The melting temperature of the treated sample was slightly increased by 0.42%; while the decomposition temperature was decreased by 7.60%, compared to the control sample. Besides, the treated sample showed alterations in the ΔH_{fusion} and $\Delta H_{decomposition}$ by 7.63% and -12.96%, respectively compared with the control sample. Hence, the thermal data of both the samples indicated that the thermal stability of the treated sample was increased, compared to the untreated ascorbic acid sample. Hence, the overall results on the Biofield Energy Treated ascorbic acid revealed the impact of the Trivedi Effect®-Consciousness Energy Healing Treatment on the physicochemical and thermal properties involving the crystalline properties, particle sizes, surface area, thermal degradation, and melting profile, etc. The Biofield Energy Treatment of the sample might form a new polymorph of the ascorbic acid that may show better appearance, flowability, content uniformity and efficacy along with improved thermal stability compared to the untreated sample. Thus, it could be concluded that the Biofield Energy Treated ascorbic acid could be used in the nutraceutical/pharmaceutical formulation for providing better prevention and treatment against various diseases such as scurvy, tuberculosis, common cold, febrile states, hypercholesterolemia, pneumonia infection, coronary heart disease, whooping cough, rheumatic fever, hypertension, angina pectoris, congestive cardiac failure, diphtheria, vascular disorders, diabetes mellitus and sinusitis, glaucoma, autoimmune diseases, bleeding gums, neurotic disturbances, and may improve the fracture, burns and wound healing, etc.

ACKNOWLEDGEMENT

The authors are grateful to Central Leather Research Institute, SIPRA Lab. Ltd., Trivedi Science, Trivedi Global, Inc., Trivedi Testimonials, and Trivedi Master Wellness for their assistance and support during this work.

REFERENCES

1. Buettner GR, Jurkiewicz BA (1996) Catalytic metals, ascorbate and free radicals: Combinations to avoid. Radiat Res 145: 532-541.
2. Lykkesfeldt J, Michels AJ, Frei B (2014) Vitamin C. Adv Nutr 5: 16-18.

3. Englard S, Seifter S (1986) The biochemical functions of ascorbic acid. Annu Rev Nutr 6: 365-406.

4. Malo C, Wilson JX (2000) Glucose modulates vitamin C transport in adult human small intestinal brush border membrane vesicles. J Nutr 130: 63-69.

5. Heitzer T, Schlinzig T, Krohn K, Meinertz T, Münzel T (2001) Endothelial dysfunction, oxidative stress, and risk of cardiovascular events in patients with coronary artery disease. Circulation 104: 2673-2678.

6. Evans JR, Henshaw K (2008) Antioxidant vitamin and mineral supplements for preventing age-related macular degeneration. Cochrane Database Syst Rev CD000253.

7. Mandl J, Szarka A, Bánhegyi G (2009) Vitamin C: update on physiology and pharmacology. Br J Pharmacol 157: 1097-1110.

8. Rowan MP, Cancio LC, Elster EA, Burmeister DM, Rose LF, et al. (2015) Burn wound healing and treatment: review and advancements. Crit Care 19: 243.

9. Figueroa-Méndez R, Rivas-Arancibia S (2015) Vitamin C in health and disease: Its role in the metabolism of cells and redox state in the brain. Front Physiol 6: 397.

10. Miranda A, Caraballo I, Millán M (2002) Stability study of flutamide in solid state and in aqueous solution. Drug Dev Ind Pharm 28: 413-422.

11. Anjum S, Swan SK, Lambrecht LJ, Radwanski E, Cutler DL, et al. (1999) Pharmacokinetics of flutamide in patients with renal insufficiency. Br J Clin Pharmacol 47: 43-47.

12. Frass M, Strassl RP, Friehs H, Müllner M, Kundi M, et al. (2012) Use and acceptance of complementary and alternative medicine among the general population and medical personnel: A systematic review. Ochsner J 12: 45-56.

13. Barnes PM, Bloom B, Nahin RL (2007) Complementary and alternative medicine use among adults and children: United States, 2007. Natl Health Stat Report 12: 1-23.

14. Rubik B (2002) The biofield hypothesis: Its biophysical basis and role in medicine. J Altern Complement Med 8: 703-717.

15. Koithan M (2009) Introducing complementary and alternative therapies. J Nurse Pract 5: 18-20.

16. Berman JD, Straus SE (2004) Implementing a research agenda for complementary and alternative medicine. Annu Rev Med 55: 239-254.

17. Trivedi MK, Branton A, Trivedi D, Nayak G, Nykvist CD, et al. (2017) Evaluation of the Trivedi Effect® - Energy of consciousness energy healing treatment on the physical, spectral and thermal properties of zinc chloride. Am J Life Sci 5: 11-20.

18. Trivedi MK, Patil S, Shettigar H, Bairwa K, Jana S (2015) Spectroscopic characterization of biofield treated metronidazole and tinidazole. Med Chem 5: 340-344.

19. Trivedi MK, Branton A, Trivedi D, Shettigar H, Bairwa K, et al. (2015) Fourier transform infrared and ultraviolet-visible spectroscopic characterization of biofield treated salicylic acid and sparfloxacin. Nat Prod Chem Res 3: 186.

20. Trivedi MK, Patil S, Shettigar H, Mondal SC, Jana S (2015) Evaluation of biofield modality on viral load of Hepatitis B and C viruses. J Antivir Antiretrovir 7: 83-88.

21. Trivedi MK, Patil S, Shettigar H, Mondal SC, Jana S (2015) An impact of biofield treatment: Anti-mycobacterial susceptibility potential using BACTEC 460/MGIT-TB System. Mycobact Dis 5: 189.

22. Trivedi MK, Branton A, Trivedi D, Nayak G, Charan S, et al. (2015) Phenotyping and 16S rDNA analysis after biofield treatment on *Citrobacter braakii*: A urinary pathogen. J Clin Med Genom 3: 129.

23. Trivedi MK, Branton A, Trivedi D, Nayak G, Mondal SC, et al. (2015) Morphological characterization, quality, yield and DNA fingerprinting of biofield energy treated alphonso mango (*Mangifera indica* L.). J Food Nutr Sci 3: 245-250.

24. Trivedi MK, Branton A, Trivedi D, Nayak G, Mondal SC, et al. (2015) Evaluation of biochemical marker-Glutathione and DNA fingerprinting of biofield energy treated *Oryza sativa*. Am J BioSci 3: 243-248.

25. Trivedi MK, Branton A, Trivedi D, Nayak G, Mondal SC, et al. (2015) Effect of biofield treated energized water on the growth and health status in chicken (*Gallus gallusdomesticus*). Poult Fish WildlSci 3: 140.

26. Trivedi MK, Tallapragada RM, Branton A, Trivedi D, Nayak G, et al. (2015) The potential impact of biofield energy treatment on the physical and thermal properties of silver oxide powder. Int J Biomed Sci Eng 3: 62-68.

27. Trivedi MK, Tallapragada RM, Branton A, Trivedi D, Nayak G, et al. (2015) Analysis of physical, thermal, and structural properties of biofield energy treated molybdenum dioxide. Int J Mater Sci Appl 4: 354-359.

28. Nayak G, Altekar N (2015) Effect of biofield treatment on plant growth and adaptation. J Environ Health Sci 1: 1-9.

29. Kinney JP, Trivedi MK, Branton A, Trivedi D, Nayak G, et al. (2017) Overall skin health potential of the biofield energy healing based herbomineral formulation using various skin parameters. Am J Life Sci 5: 65-74.

30. Smith DM, Trivedi MK, Branton A, Trivedi D, Nayak G, et al. (2017) Skin protective activity of consciousness energy healing treatment based herbomineral formulation. J Food Nutr Sci 5: 86-95.

31. (1997) Desktop X-ray Diffractometer "MiniFlex+". Rigaku J 14: 29-36.

32. Zhang T, Paluch K, Scalabrino G, Frankish N, Healy AM, et al. (2015) Molecular structure studies of (1S,2S)-2-benzyl-2,3-dihydro-2-(1Hinden-2-yl)-1H-inden-1-ol. J Mol Struct 1083: 286-299.

33. Langford JI, Wilson AJC (1978) Scherrer after sixty years: A survey and some new results in the determination of crystallite size. J Appl Cryst 11: 102-113.

34. Trivedi MK, Sethi KK, Panda P, Jana S (2017) Physicochemical, thermal and spectroscopic characterization of sodium selenate using XRD, PSD, DSC, TGA/DTG, UV-vis and FT-IR. Marmara Pharm J 21/2: 311-318.

35. Trivedi MK, Sethi KK, Panda P, Jana S (2017) A comprehensive physicochemical, thermal and spectroscopic characterization of zinc (II) chloride using X-ray diffraction, particle size distribution, differential scanning calorimetry, thermogravimetric analysis/differential thermogravimetric analysis, ultraviolet-visible and Fourier transform-infrared spectroscopy. Int J Pharm Investig 7: 33-40.

36. Trivedi MK, Branton A, Trivedi D, Nayak G, Plikerd WD, et al. (2017) A systematic study of the biofield energy healing treatment on physicochemical, thermal, structural and behavioral properties of iron sulphate. Int J Bioorg Chem 2: 135-145.

37. Trivedi MK, Branton A, Trivedi D, Nayak G, Lee AC, et al. (2017) Evaluation of the impact of biofield energy healing treatment (The Trivedi Effect®) on the physicochemical, thermal, structural and behavioural properties of magnesium gluconate. Int J Nutr Food Sci 6: 71-82.

38. Trivedi MK, Branton A, Trivedi D, Nayak G, Plikerd WD, et al. (2017) Evaluation of the physicochemical, spectral, thermal and behavioral properties of sodium selenate: Influence of the energy of consciousness healing treatment. Am J Quantum Chem Mol Spectroscopy 2: 18-27.

39. Savjani KT, Gajjar AK, Savjani JK (2012) Drug solubility: Importance and enhancement techniques. ISRN Pharmaceutics, Article ID 195727.

40. Morin G, Briens L (2013) The effect of lubricants on powder flowability for pharmaceutical application. AAPS Pharm Sci Tech 14: 1158-1168.

41. Hlinak AJ, Kuriyan K, Morris KR, Reklaitis GW, et al. (2006) Understanding critical material properties for solid dosage form design. J Pharm Innov 1: 12-17.

42. Nunes JFL, Melo DMA, de Moura MFV, de Farias RF (2007) TG-DSC study of ascorbic acid pharmaceutical formulations: Sodium croscarmellose, microcrystalline cellulose and lactose as excipients. Revista Química no Brasil 1: 7-14.

43. Zhao Z, Xie M, Li Y, Chen A, Li G, et al. (2015) Formation of curcumin nanoparticles via solution enhanced dispersion by supercritical CO_2. Int J Nanomed 10: 3171-3181.